Aerodynamically Accurate Three-Dimensional Navier–Stokes Method

B. Epstein,* A. Jacobs,† and A. Nachshon*
Israel Aircraft Industries, Lod 70100, Israel

I. Introduction

THERE is insufficient use of Navier–Stokes methods in the aircraft industry for practical purposes. To overcome this, the aerodynamic accuracy of the method, that is, the ability to estimate important characteristics such as lift and drag, must be proven. The present work improves the accuracy by means of a numerical approach that does not employ any explicit artificial dissipation.

A numerical method for the compressible Navier–Stokes equations is presented. It is the basis of the three-dimensional NES code (verified for two-dimensional flows[1]), intended to deal with practical configurations similarly to MGAERO.[2] The algorithm [based on the essentially nonoscillatory (ENO) approach introduced by Harten et al.[3] and Shu and Osher[4]] is implemented by the finite volumes method in physical space on grids defined by a set of vertices. Nonlinear stability is maintained by approximating inviscid fluxes on a variable template. A specially constructed algorithm diminishes considerably the amount of computation associated with changeability of template. Results include 1) a test case of the ONERA-M6 wing and 2) transonic flow over a realistic transport type cranked wing with highly cusped profiles. The comparisons with experiment indicate good accuracy on relatively coarse grids.

II. Numerical Method

Integrating the Navier–Stokes equations in Cartesian coordinates over a particular cell of an (i, j, k) structure, the following approximation is assumed:

$$\begin{aligned}(\Omega_{i,j,k}\, \boldsymbol{q}_{i,j,k})_t &+ [\boldsymbol{C} \cdot (S\boldsymbol{n})]_{i+0.5,j,k} - [\boldsymbol{C} \cdot (S\boldsymbol{n})]_{i-0.5,j,k} \\ &+ [\boldsymbol{C} \cdot (S\boldsymbol{n})]_{i,j+0.5,k} - [\boldsymbol{C} \cdot (S\boldsymbol{n})]_{i,j-0.5,k} \\ &+ [\boldsymbol{C} \cdot (S\boldsymbol{n})]_{i,j,k+0.5} - [\boldsymbol{C} \cdot (S\boldsymbol{n})]_{i,j,k-0.5} \\ &= [\boldsymbol{V} \cdot (S\boldsymbol{n})]_{i+0.5,j,k} - [\boldsymbol{V} \cdot (S\boldsymbol{n})]_{i-0.5,j,k} + \cdots \end{aligned} \tag{1}$$

where $\Omega_{i,j,k}$ is the cell volume, $\boldsymbol{q}_{i,j,k}$ is some mean value of the solution $\boldsymbol{q}$ over the cell, $\boldsymbol{C}$ and $\boldsymbol{V}$ approximate, respectively, convection and viscous terms, and S is the area of a cell side surface. Half-indices indicate on which side of the cell a flux is taken. Inviscid fluxes with half-indices are approximated by those given at the cell centers one dimensionally, i.e., fluxes with subscripts $I + 0.5$, J, K and $I - 0.5$, J, K are approximated by fluxes at the cell centers with constant J and K and so on. The interpolation operator I must be exact for a constant-field solution, which is ensured by choosing it in the form

$$[\boldsymbol{C} \cdot (S\boldsymbol{n})]_{i+0.5,j,k} = I\{\boldsymbol{C}_{I,j,k} \cdot (S\boldsymbol{n})_{i+0.5,j,k}\}_{I=i,i+1,i-1,\ldots} \tag{2}$$

with the direction vector frozen in the interpolant. Fluxes in the right-hand side of Eq. (2) are projected into local characteristic fields. A template (typically consisting of three points) is determined separately in each field, primarily according to the sign of the corresponding eigenvalue and then according to the smoothness of the projected fluxes (see Refs. 1, 3, and 4 for more details). Viscous fluxes are approximated in a straightforward way. Time marching uses a three-stage Runge–Kutta scheme applied in a total variation diminishing preserving form.[4] To accelerate the convergence to steady state, explicit residual smoothing is applied, allowing Courant–Friedrichs–Lewy numbers of about 1.5, and local time steps are used.

New templates are determined only once for all three Runge–Kutta stages, and a linearly stable template is applied everywhere except in the neighborhood of sensitive cell faces, where the variable ENO template is applied (the cell face is called sensitive if one of the sonic eigenvalues changes sign across the face, the neighborhood being determined by the number of points in the ENO template minus 1).

The code is embedded in the framework of the multigrid method with local refinements. Because of the limited computer resources available (IBM RS6000/580), most runs have been performed in the framework of Full MultiGrid.

III. Results and Discussion

Solutions for transonic flow over two different wing configurations are presented. C–O grid topologies are used. Normal spacing at the wing surface ensure y^+ of about 1.5–2.5 on fine meshes. The effects of turbulence are modeled through the Baldwin–Lomax model.

ONERA-M6 Wing

The computed pressure distributions are in close agreement with experiment[5] at $M_\infty = 0.84$ and $\alpha = 3.06$ deg along the whole wing span. Figure 1 shows the pressure coefficients at $2y/b = 0.44$ and (the particularly difficult flow) at $2y/b = 0.78$, where good shock capturing capability is needed in both the streamwise and spanwise directions. A reasonably converged solution employing three successive grids, $44 \times 16 \times 8$, $88 \times 16 \times 16$, and $176 \times 24 \times 16$, yields values of $C_L = 0.268$ and $C_D = 0.0178$. These are almost identical to the results of Refs. 6 and 7, where grids consisted of $269 \times 65 \times 49$ points.

Transport Type Cranked Wing

In this configuration, the transonic flowfield is highly influenced by shock/boundary-layer interaction. The twisted wing with highly cusped profiles is part of a transport type aircraft that was the subject of several numerical studies[2,8] that gave a satisfactory picture in the low transonic regime but failed at more demanding flight conditions. Grids contain up to $176 \times 32 \times 16$ points. Reynolds number is 3.0×10^6.

Typical lift curve and lift/drag polar are compared with experiment at $M_\infty = 0.75$ in Fig. 2, where the experimental drag represents the difference between the wing–body and the body-only drag values. The computational and experimental lift curves possess almost identical slopes along the whole range of α but are shifted by about 0.4 deg (due, perhaps, to the influence of a wing–body fairing present in the experiment but missing in the stand-alone wing computations). The computational lift/drag polar is in close agreement with experiment, including the value of the zero lift drag coefficient.

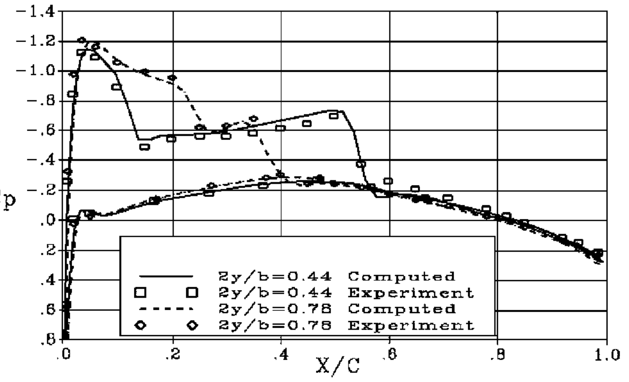

Fig. 1 Chordwise Cp distribution at $M_\infty = 0.84$, $\alpha = 3.06$ deg at $2y/b = 0.44$ and 0.78, ONERA-M6.

Received Aug. 12, 1996; revision received Jan. 15, 1997; accepted for publication Feb. 12, 1997.

*Research Scientist, Computational Fluid Dynamics Group, Department 4473, Engineering Center, Ben-Gurion Airport.

†Research Scientist, Computational Fluid Dynamics Group, Department 4473, Engineering Center, Ben-Gurion Airport. E-mail: ajacobs@eng-div.iai.co.il.

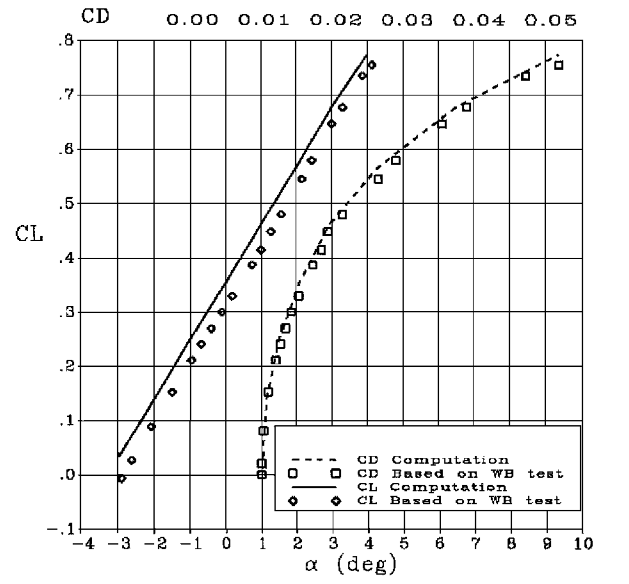

Fig. 2 Lift coefficient curve and lift/drag polar at $M_\infty = 0.75$ and $Re = 3.5 \times 10^6$, transport type wing.

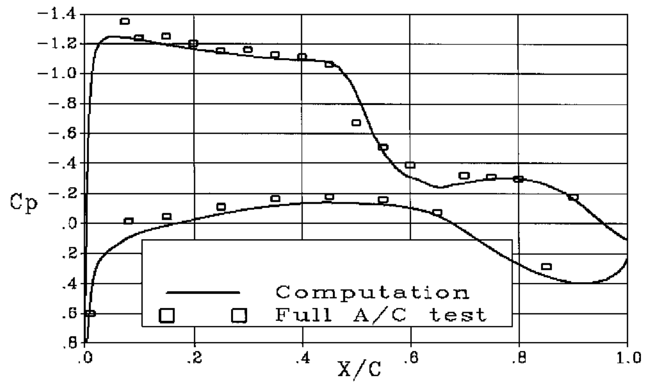

a) $M_\infty = 0.80$

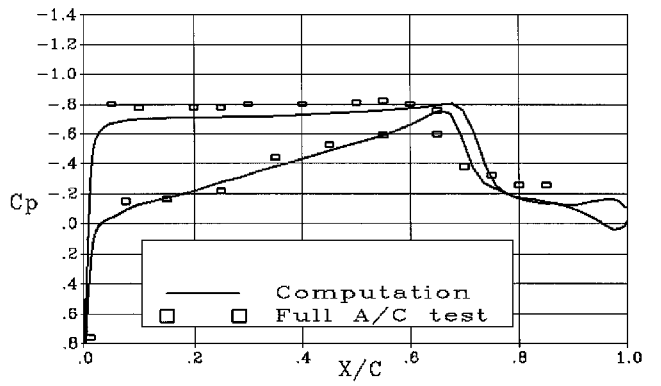

b) $M_\infty = 0.92$

Fig. 3 Chordwise *Cp* distribution at $2y/b = 0.65$ at fixed angle of attack, $Re = 3.5 \times 10^6$, transport type wing.

Pressure comparisons are given for $M_\infty = 0.80$ and 0.92 at the span section $2y/b = 0.65$ at a fixed experimental angle of attack (Fig. 3). The pressure experiment included the full aircraft, and so the computational angle of attack was adjusted to ensure an approximately correct wing loading in the case of $M_\infty = 0.80$ (with C_L close to that of cruise) and then kept unchanged for $M_\infty = 0.92$. Shocks are properly captured, and (in the case of $M_\infty = 0.92$) the destructive flow separation from the lower surface is described correctly.

IV. Convergence and Accuracy

ENO schemes maintain (nonlinear) stability by varying the computational template where necessary. As a result, the traditional picture of the maximum residuals diminishing up to machine zero vanishes. We refrained from using additional numeric parameters to overcome this inconvenience in order to avoid an undesirable back door introduction of artificial dissipation. The convergence is estimated, together with the reduction of residuals by several orders of magnitude, by the steadiness of the solution (negligibility of variations in the computed flow characteristics). In fact, the level of the variations reflects the ability of a grid to resolve the flow properly, thus supplying guidelines for necessary grid refinement. In the described runs, the L_1 norm of the continuity equation has been reduced by 3–4 orders of magnitude, allowing roughly 3 significant figures in lift and pressure drag coefficients.

V. Concluding Remarks

A numerical method and a corresponding computer code for solving the compressible Navier–Stokes equations are presented, based on an ENO finite volumes method. Because of its low-dissipation scheme, the method achieves good engineering accuracy on relatively coarse grids, thus ensuring the overall favorable cost effectiveness.

References

[1]Epstein, B., and Nachshon, A., "An ENO Navier–Stokes Solver Applied to 2-D Subsonic, Transonic and Hypersonic Flows," AIAA Paper 94-0303, Jan. 1994.

[2]Epstein, B., Luntz, A. L., and Nachshon, A., "Cartesian Euler Method for Arbitrary Aircraft Configurations," *AIAA Journal*, Vol. 30, No. 3, 1992, pp. 679–687.

[3]Harten, A., Engquist, B., Osher, S., and Chakravarthy, S., "Uniformly High Order Accurate Non-Oscillatory Schemes, I," *Journal of Computational Physics*, Vol. 71, No. 2, 1987, pp. 231–303.

[4]Shu, C.-W., and Osher, S., "Efficient Implementation of Essentially Non-Oscillatory Shock-Capturing Schemes," *Journal of Computational Physics*, Vol. 83, No. 1, 1989, pp. 32–78.

[5]Schmitt, V., and Charpin, F., "Pressure Distributions on the ONERA-M6 Wing at Transonic Mach Numbers," AGARD-AR-138, May 1979.

[6]Radespiel, R., and Rossow, C., "An Efficient Cell-Vertex Multigrid Scheme for the Three-Dimensional Navier–Stokes Equations," AIAA Paper 89-1953, June 1989.

[7]Turkel, E., and Vatsa, V. N., "Effect of Artificial Viscosity on Three-Dimensional Flow Solutions," *AIAA Journal*, Vol. 32, No. 1, 1994, pp. 39–45.

[8]Epstein, B., Luntz, A. L., and Nachshon, A., "Multigrid Transonic Computations About Arbitrary Aircraft Configurations," *Journal of Aircraft*, Vol. 26, No. 8, 1989, pp. 751–759.

J. Kallinderis
Associate Editor